

DESICCATION SHRINKAGE AND ITS CONTROLLING PROPERTIES: MULTIPHYSICS

L.B. HU^{*#}, T. HUECKEL^{*}, H. PERON[&] AND L. LALOU[&]

^{*}Duke University,
Civil and Environmental Engineering Department
Durham, NC 27514, USA
hueckel@duke.edu

[#] currently University of Vermont, VT, USA
Civil and Environmental Engineering
213 Votey, 33 Colchester Ave. Burlington, VT 05405-0156
lh19@duke.edu

[&]EPFL, Lausanne, Switzerland
ENAC, Station 18, CH-1015 Lausanne, Switzerland
herve.peron@epfl.ch, lvesse.laloui@epfl.ch

Summary *We examine the pore space evolution during saturated stage of soil drying as obtained via porosimetry. This is modeled at a microscale using Poiseuille flow through the capillary vessels of the size of the actual modal pores, with deformable walls driven by evaporation flux at the external boundary. Onset of desaturation and the post-saturation stage are subsequently simulated as water cavitation mechanism and moving liquid/vapor interface inside the pores.*

Key words: desiccation, evaporation, shrinkage, multiphysics, porosimetry, modeling

1 INTRODUCTION

Recent desiccation experiments (Peron et al.¹) on initially saturated soils near liquid limit point out to the conclusion that most of the shrinkage occurs during saturated phase of the process. This is in agreement with a general perception that unsaturated soil has a much higher stiffness than saturated soil, so it deforms much less. This is quite a universal behavior independently of the type of soil and type of pore fluid, as shown by Hu et al.², including soils permeated with ethanol, with surface tension half of that of water.

It was also shown that the accumulated deformation during the saturated drying and the shrinkage limit in terms of void ratio depend on the compressibility of the solid, and surface tension and/or fluid saturation vapor pressure which characterizes the evaporation process, or finally, of fluid viscosity. However, the rate of fluid loss and rate of shrinking are controlled by the evaporative and hydraulic conductivity properties, thus, those of the fluid.

2 PORE SPACE EVOLUTION MODELING

A microscopic model of pore system deformation and transport is proposed to corroborate the above hypothesis in relationship to the actual data on the evolution of the pore space. Pore size distribution was obtained using Mercury Intrusion Porosimetry at the water content of 33.1%, 24.8% and at 0.8%, corresponding to the initial state, a state near shrinkage limit, and a practically dry state **indicate that**: (1) the initial pore size distribution is visibly bi-modal, with Large Pores (LP), ranging between $0.6\mu\text{m}$ and $3\mu\text{m}$ occupying initially 17% of the volumes of the medium, and Small Pores (SP), ranging between $0.09\mu\text{m}$ and $0.6\mu\text{m}$ occupying initially 21% of the volume of the medium; (2) Near shrinkage limit the LP take less than 5% of the volume of the medium, whereas the SP amount to 29%; (3) Near the completion of drying, the LPs take less than 0.5% of the volume of the medium, whereas the SP still amount to 27%. It is hence concluded that the Small Pores do not decrease significantly, neither in size nor in total volume they occupy.

The model of an evolving microscopic structure is made of straight tubes of two initial sizes: small (SP) and large (LP), with their internal diameters coinciding with the average values of the modal pores of $0.5\mu\text{m}$ and $1\mu\text{m}$. The total initial volume of the pores is equal to the initial value of the total modal pore volumes. The external radii of the tubes, $2.5\mu\text{m}$, are calculated by equating the volume of the solids of all the tubes to the total volume of solids.

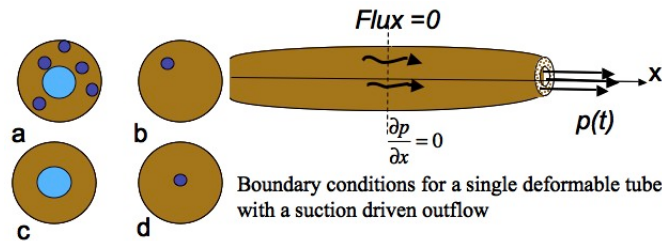


Figure 3. Schematics of the pore system

A representative elementary volume (REV) is in a form of a single cylindrical deformable tube around a central cylindrical LP and twelve parallel SPs, all filled with water, and connected at their extremities to the atmosphere and exchanging gas and fluid. The behavior of the solids around the pores is considered plastic, approximated via a linear stress-strain law during loading and perfectly rigid during an unloading. The linearity of deformation law allows one to represent the response of the pore system of Fig. 1 as a superposition of effects of an LP and multiple SPs. For the reasons of simplicity SPs are located centrally as well. Hence, the problem is reduced to that of a single tube with a single cylindrical pore.

The tube is considered as symmetric along and around its axis, initially filled with water during saturated phase. Water inside the pore undergoes a viscous (Poiseuille) flow. The external boundary conditions consist in a known water pressure (negative) history, or an imposed flux, resulting from the evaporation flux. The removal of water from the tube implies that its volume change is compensated by the deformation of the tube. The problem is described by a parabolic PDE

$$\frac{\partial^2 p}{\partial x^2} + \frac{2a_0}{Eh \left[1 - \frac{pa_0}{Eh} \right]} \left(\frac{\partial p}{\partial x} \right)^2 = \frac{16\mu}{a} \frac{\left[1 - \frac{pa_0}{Eh} \right]}{Eh} \frac{\partial p}{\partial t} \quad (1)$$

The initial condition is: at $t = 0$, $p = p_0 = 0$. The boundary conditions are as follows: $x = 0$, $\partial p / \partial x = 0$ and $x = \pm L$, $p = p(t)$. The solution has been obtained using Matlab[®].

3 RESULTS

The solutions are obtained for large and small pores separately. The numerical value of the deformability modulus $E = 50$ KPa, and water viscosity are chosen the same for the analyses of the LP and the SPs. The length of the tubes is 15 cm. Both types of pores are subjected to the same external negative pressure evolution, as resulting from the same flux of water vapor (see Hu et al.¹). The most significant difference between the two types of pores is in the

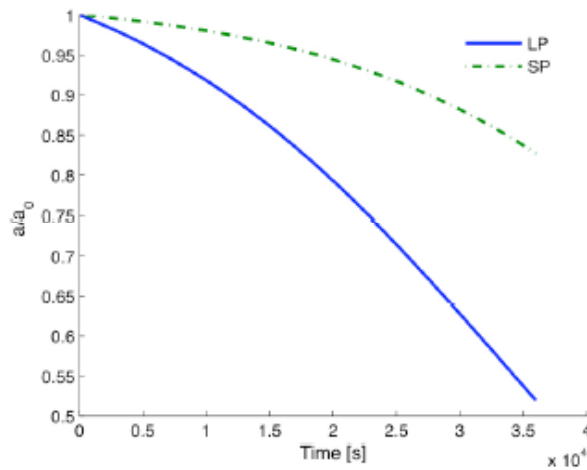


Fig. 2 Change in the normalized pore entrance size in time for Large and Small modal pore -simulation

amount of closure of the inner cavity, see Fig. 2.: in 5 hours needed for reaching the shrinkage limit, the LP closure amounts to $0.33 \mu\text{m}$ from $1 \mu\text{m}$, whereas the SP closes over $0.08 \mu\text{m}$ from the original $0.5 \mu\text{m}$ at the external boundary. This reflects the porosimetry results. SPs cavitate much later than LPs, as it depends on the pore size. The post cavitation stage consists mainly in the water removal as evaporation localized at the liquid/vapor interface, inducing suction driven water transport towards the interface. At some point the water gradient disappears in the water filled portion of the tube and water is removed solely via interface displacement, until all water is extracted. Further water removal occurs through the same mechanisms in SPs. Interestingly, the stage after the cavitation generates almost no shrinkage.

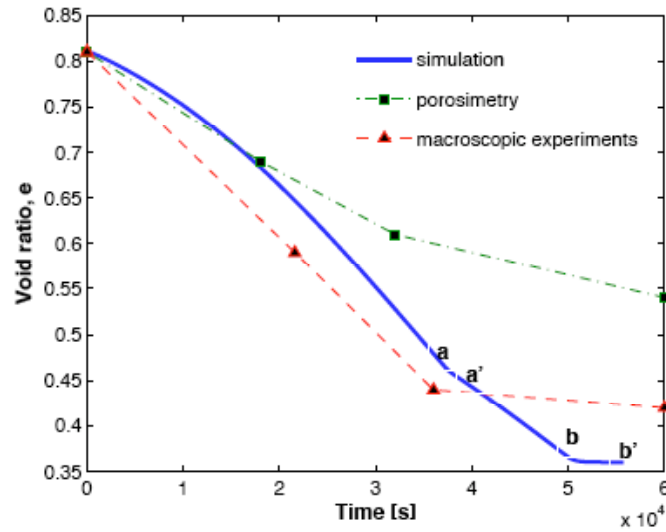


Fig. 3. Total change in void ratio: Simulation compared to the experimental data from porosimetry and macroscopic measurement: a- cavitation in LP, a'-end of fluid flow inLP (no pressure gradient); similar events in SPs are marked by b and b'

Clearly, the obtained evolution is simplified by the choice of two modal pores only. The picture could be made more realistic by considering many more pore sizes. Also, quite strong is the hypothesis of a total removal of water from a portion of the tube beyond the interface, without any local capillary effects, and hence any pressure in this segment.

4 CONCLUSIONS

There is a quantitative support for the hypothesized mechanisms triggered by drying. It is concluded that the driving force at the initial stage is Poiseuille water flow in pore conduits induced by the liquid water removal via phase transition at the boundary. The water removal generates a negative water pressure, and its gradient along the pore vessels generates water flow. Deformation of the porous vessels compensates for the mass removal of water from the vessels. The pressure (suction, to be exact) and pressure gradient is imposed by the evaporation rate, and hence boundary water removal whereas the deformation is controlled by the deformability of the solids alone. The shrinkage rate is controlled by the fluid viscosity, evaporation rate and experimentally measured variable pore radii.

REFERENCES

- [1] Peron, H., Laloui, L., Hueckel, T. & Hu, L.B. 2006. Experimental study of desiccation of soil. G.A. Miller et al. (eds.), *ASCE Geotechn. Sp.Publ. 147: Unsaturated Soils 2006*, 1073-84
- [2] Hu, L.B., Peron, H., Hueckel, T. & Laloui, L. 2007. Drying shrinkage of deformable porous media: mechanisms induced by the fluid removal, H.W. Olson (ed.), *ASCE Geotechn. Sp.Publ. 157: Geo-Denver 2007*